Appl. Phys. B 39, 141–147 (1986)

Applied Physics B Photophysics and Laser Chemistry

Polarization Effects of Picosecond CARS in Liquids

N. Kohles and A. Laubereau

Physikalisches Institut, Universität, D-8580 Bayreuth, Fed. Rep. Germany

Received 14 November 1985/Accepted 25 November 1985

Abstract. Coherent Raman scattering of delayed probing pulses after ultrafast excitation is investigated under generalized polarization conditions. Three factors are shown to contribute to the scattering signal:
(i) scattering off the isotropic part of the resonant material excitation via the isotropic component of the Raman polarizability
(ii) scattering via the anisotropic part of the Raman polarizability from a second, oriented component of the resonant material excitation
(iii) four-wave mixing via the non-resonant part χ_{NR} of the third-order susceptibility.
We demonstrate theoretically and experimentally that different polarization conditions lead to drastic changes of the signal transients in liquids. For the ring breathing mode of C_6H_5Br the ratio of non-resonant to resonant contributions is measured to be $\chi_{NR}/\chi_{res} = 0.037 \pm 0.015$.

PACS: 42.65.Cq, 78.30.Cp

Ultrafast excitation and subsequent probing of molecular vibrations in liquids and gases and of lattice vibrations in solids have received increasing interest in recent years [1, 2]. Two synchronized pulses of picosecond or subpicosecond duration and proper frequency difference drive the vibrational transition of interest close to resonance. The vibrational excitation is monitored by coherent Stokes or anti-Stokes scattering of delayed probing pulses. In numerous investigations this time-domain spectroscopy was used to study the dephasing of molecular vibrations [3] or to determine the phonon lifetimes of lattice modes [4, 5]. It has been also shown that information can be obtained on different parts of the third-order nonlinear susceptibility $\chi^{(3)}$, e.g. separating resonant and non-resonant contributions [6, 7]. Very recently a Fourier transform technique has been demonstrated for picosecond CARS of supersonic expansions achieving high frequency resolution of $10^{-3}\,cm^{-1}$ [8].
Previous work on liquids has been performed under special polarization conditions with parallel polarization of the excitation pulses. These studies provided information on vibrational dephasing. The present paper is devoted to more general situations. Theoretical and experimental data will be presented demonstrating that the observed signal transients and the obtained information are vastly different depending on the specific polarization conditions for the liquid case. This fact is connected to the varying contributions of molecular rotation and of non-resonant four-photon interaction to the measuring process. For solids with essentially frozen molecular orientations the situation is different [7] and will not be discussed in the following.

Theory

The theoretical treatment of coherent Raman probing is well established for parallel polarization of the exciting laser and Stokes pulses (electric field amplitudes $E_L, E_S, E_L \| E_S$). Correspondingly, the anti-Stokes scattering (E_A) of the delayed probing pulse (E_P) was also discussed for parallel direction, $E_A \| E_p$ [9]. In experimental studies the angle between the polarization planes of the excitation and probing process has been often chosen to be 90° for practical reasons. This polarization geometry is depicted in Fig. 1 as case 1a. Figure 1 also includes the situation with all four field vectors parallel (case 1b). More general conditions with arbitrary angle between the pairs of pulses for

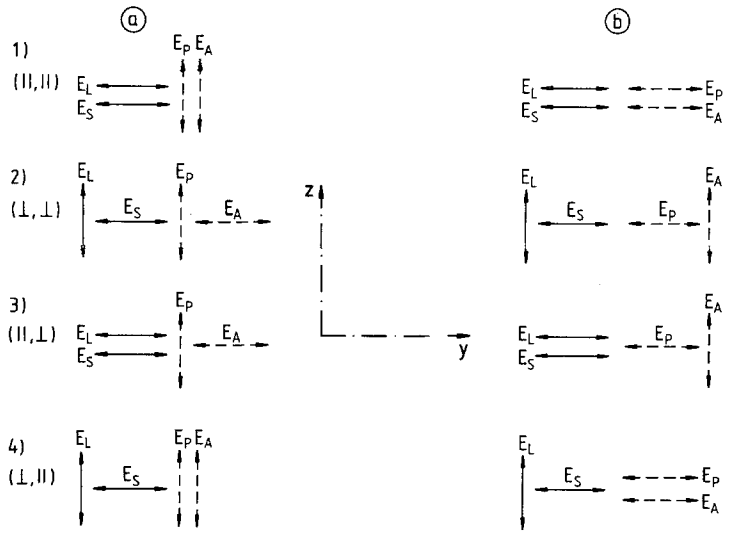

Fig. 1a and b. Polarization geometries of coherent Raman scattering; E_L, E_S: excitation pulses; E_P, E_A: incident and scattered probe field

excitation and probing may be represented by a linear superposition of the two parallel cases 1a and 1b. These situations (||, ||) will be referred to as "parallel polarization".

Physically different is the situation with perpendicular polarization planes of the two excitation pulses $E_L \perp E_S$, and correspondingly also of the two probe field components $E_p \perp E_A$. Such polarization conditions (⊥, ⊥) will be termed crossed polarization in the following. Two specific situations of this kind are shown in Fig. 1 as cases 2a and 2b. Case 2b differs from case 2a by a rotation of the probe fields by 90°. For general pump and probe experiments finally the question arises if parallel pump polarization may be combined with perpendicular probe polarization (||, ⊥) and vice versa (⊥, ||). Four cases of this kind, which will be called mixed polarization, are also depicted in the figure. The examples of Fig. 1 are restricted to linearly polarized fields. The general case of coherent probe scattering involving four fields of elliptical polarization may be evaluated by a superposition of the various situations of Fig. 1 [9].

Our theoretical discussion adopts the notation of [2]. We consider an approximately collinear geometry with linearly polarized light pulses propagating in the x-direction. Without loss of generality, the input Stokes pulse is assumed to be polarized in the y-direction. The interaction between the electromagnetic field and the vibrational transition is described by the Raman polarizability tensor $(\partial\alpha/\partial q)$. We restrict the discussion to molecules with axial symmetry, where only two quantities, the isotropic part, a, and the anisotropic part γ of $(\partial\alpha/\partial q)$ have to be considered.

The orientation of the molecular symmetry axis is treated purely classically and represented by the direction cosines $\cos\theta_1$, $\cos\theta_2$, and $\cos\theta_3$ with respect to the x, y, and z axis of the laboratory frame. In liquids the angles θ_i are rapidly changing functions of time. Following [2] the amplitudes of the resonant part of the nonlinear polarization connected to the vibrational excitation are evaluated to be

$$P_{\parallel}^{\mathrm{res}} = E_p N a \langle Q s_1 \rangle \tag{1a}$$

and

$$P_{\perp}^{\mathrm{res}} = E_p N a \langle Q s_2 \rangle . \tag{1b}$$

$P_{\parallel}^{\mathrm{res}}(P_{\perp}^{\mathrm{res}})$ denotes the component parallel (perpendicular) to the linearly polarized probe field E_p. The brackets $\langle\ \rangle$ represent ensemble averages over the orientational distribution. Q is the amplitude factor of the expectation value of the normal mode operator and represents the coherent vibrational excitation. s_1, s_2 are time-dependent factors containing the ratio γ/a of the coupling parameters and the direction cosines

$$\begin{aligned} s_1(t) &= 1 + \frac{\gamma}{a}(\cos^2\theta_3 - \tfrac{1}{3}), \\ s_2(t) &= \frac{\gamma}{a}\cos\theta_2 \cos\theta_3 . \end{aligned} \tag{2}$$

We note that the molecular orientation enters the calculation only for a non-vanishing anisotropy $\gamma/a \neq 0$. The non-resonant contribution to the nonlinear polarization is written by the help of the non-resonant part χ_{NR} of the third-order susceptibility tensor.

Evaluating a two-level model we find the vibrational excitation produced by the pump fields E_L and E_S $(j = 1, 2)$.

$$\begin{aligned} \langle Q s_j \rangle = \kappa_2 \int_{-\infty}^{t} dt' \exp[(t'-t)/T_2 - \mathrm{i}\Delta\omega t'] E_L(t') \\ \cdot [E_{S\parallel}^{*} \langle s_j(t) s_1(t') \rangle + E_{S\perp}^{*} \langle s_j(t) s_2(t') \rangle] . \end{aligned} \tag{3}$$

The coupling coefficient κ_2 combines several material parameters. The subscripts $\|, \perp$ of E_S here indicate the Stokes field direction with respect to the pump field E_L. $\Delta\omega$ denotes the (small) frequency mismatch of the excitation fields. Assuming optical Kerr effect to be negligible (i.e., for sufficiently weak fields) the orientational average in (3) can be carried out over the equilibrium distribution. As a result, the factors $\langle s_j s_l \rangle$ in (3) may be expressed by the (equilibrium) rotational autocorrelation functions ϕ_1 and ϕ_2

$$\langle s_1(t)s_1(t')\rangle = 1 + \tfrac{4}{45}\left(\frac{\gamma}{a}\right)^2 \phi_1(t'-t),$$

$$\langle s_2(t)s_2(t')\rangle = \tfrac{1}{15}\left(\frac{\gamma}{a}\right)^2 \phi_2(t'-t), \tag{4}$$

$$\langle s_1(t)s_2(t')\rangle = \langle s_2(t)s_1(t')\rangle = 0.$$

A simple exponential time dependence will be assumed below for the rotational autocorrelation functions

$$\phi_1 \simeq \phi_2 \simeq \exp(-|t'-t|/\tau_R), \tag{5}$$

where τ_R denotes the rotational relaxation time. The different time behaviour of $\langle s_1 s_1 \rangle$ and $\langle s_2 s_2 \rangle$ should be noted according to the ratio γ/a. Inspection of (3 and 4) shows that the material excitation $\langle Q s_1 \rangle$ is produced only for parallel polarization of the pump fields E_L, E_S and depends on the correlation factor $\langle s_1 s_1 \rangle$. Similarly the excitation $\langle Q s_2 \rangle$ occurs only for perpendicular pump polarization and is related to the correlation factor $\langle s_2 s_2 \rangle$. As a result the time evolutions of $\langle Q s_1 \rangle$ and $\langle Q s_2 \rangle$ are different depending on the ratio γ/a and the rotational time constant τ_R.

For coincident laser and probe pulse of equal frequency ($\omega_L = \omega_p$) the two light pulses can interchange their roles for excitation and interrogation. Additional components of the material excitation are therefore produced ($j = 1, 2$).

$$\langle Q s_j \rangle_p = \kappa_2 \int_{-\infty}^{t} dt' \exp[(t'-t)/T_2 - i\Delta\omega t'] E_p(t_D - t') \cdot [E_{S\|}^* \langle s_j(t)s_1(t')\rangle + E_{S\perp}^* \langle s_j(t)s_2(t')\rangle]. \tag{6}$$

The subscripts $\|, \perp$ of the Stokes field here refer to the polarization of the probe pulse E_p. Scattering of the laser field E_L from the vibrational excitation of (6) leads to a coherence peak: an enhanced probe scattering signal is expected for small delay time t_D of the probe pulse [10].

Using the nonlinear wave equation and following the treatment of [2, 11] we derive the differential equation for the anti-Stokes field E_A generated by coherent Raman scattering.

Case $\|, \|$

For parallel polarization of the pump pulses, probe scattering occurs in the k-matching direction with polarization parallel to the incident probe field:

$$\frac{\partial}{\partial x'} E_{A\|} = \frac{\pi\omega_A}{\mu_A c}[(\langle Q s_1 \rangle E_p + \langle Q s_j \rangle_p E_L) N a \exp(i\Delta\omega t') + 6\,\chi_{\mathrm{NR}j} E_L E_p E_S^*]. \tag{7}$$

The subscript $j = 1$ and 2, respectively, refers to cases 1b and 1a of Fig. 1.

The $\chi_{\mathrm{NR}j}$ represent the relevant elements of the nonresonant third order susceptibility; one finds $\chi_{\mathrm{NR}1} = \chi^{\mathrm{NR}yyyy} (= \chi_{\mathrm{NR}zzzz})$ and $\chi_{\mathrm{NR}2} = \chi_{\mathrm{NR}zyzy} (= \chi_{\mathrm{NR}yzyz})$. The notation of [12] is adopted here for the nonlinear susceptibility. The factor 6 in the second term on rhs of (7) is a consequence of the frequency degeneracy $\omega_L = \omega_p$. The retarded time frame is used here with $x' = x$, $t' = t - x/v$ (group velocity v, laboratory frame x, t).

Case $\perp, \perp$

For crossed polarization planes of the excitation fields, probe scattering occurs with polarization perpendicular to the incident probe field

$$\frac{\partial}{\partial x'} E_{A\perp} = \frac{\pi\omega_A}{\mu_A c}[(\langle Q s_2 \rangle E_p + \langle Q s_j \rangle_p E_L) N a \exp(i\Delta\omega t') + 6\,\chi'_{\mathrm{NR}j} E_L E_p E_S^*], \tag{8}$$

where $j = 1$ or 2, respectively, for the polarization geometries 2b and 2a of Fig. 1. The $\chi^{(3)}$ components of interest are

$$\chi'_{\mathrm{NR}1} = \chi_{\mathrm{NR}zzyy} \; (= \chi_{\mathrm{NR}yyzz})$$

and

$$\chi'_{\mathrm{NR}2} = \chi_{\mathrm{NR}yzzy}. \tag{9}$$

Case $\|, \perp$ *and* $\perp, \|$ *(Fig. 1)*

For mixed polarization, no coherent scattering signal is predicted. This finding is a direct consequence of the approximation used in context with (4) and of the properties of the $\chi^{(3)}$ tensor of liquids. It was discussed in the literature that the isotropy of liquids require that [11]

$$\chi_{\mathrm{NR}zzzz} = \chi_{\mathrm{NR}yyzz} + \chi_{\mathrm{NR}yzyz} + \chi_{\mathrm{NR}yzzy}. \tag{10}$$

Because of the frequency degeneracy $\omega_L = \omega_p$ we have

$$\chi_{\mathrm{NR}yzyz} = \chi_{\mathrm{NR}yyzz}. \tag{11}$$

In the following we also use Kleinman's symmetry condition (applicable for negligible dispersion) which yields [13]

$$\chi_{\mathrm{NR}yzzy} = \chi_{\mathrm{NR}yzyz}. \tag{12}$$

The frequency arguments $(-\omega_A, \omega_L, \omega_L, -\omega_S)$ of the tensor elements have been omitted in (7–12) for brevity.

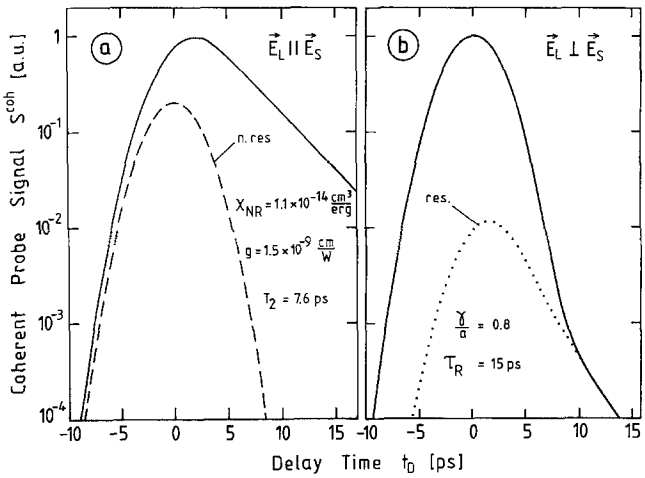

Fig. 2a and b. Calculated coherent scattering signal vs. delay time for parallel (a) and crossed (b) polarization (solid curves). Non-resonant and resonant contributions are marked by dashed and dotted lines, respectively; near-resonant excitation with frequency detuning $\Delta\omega/2\pi c = 7\,\mathrm{cm}^{-1}$; Gaussian pulses of 4.5 ps (laser) and 3 ps (Stokes); $\chi_{NR}/\chi_{res} = 0.037$; $\gamma/a = 0.8$

Experimentally the time-integrated scattering signal $S^{coh}(t_D) \propto \int_{-\infty}^{+\infty} |E_A(t_D, t')|^2 dt'$ is observed.

Some calculated results are presented in Fig. 2. A strongly polarized Raman transition equivalent to a small anisotropy of the scattering tensor ($\varrho_s = 0.04$, $\gamma/a = 0.8$) with dephasing time $T_2 = 7.6$ ps and a rather slow rotational motion ($\tau_R = 15$ ps) is considered. Parameter values of $g = 1.5 \times 10^{-9}$ cm/W (steady-state gain factor) and $\chi_{NRyzzy} = 1.1 \times 10^{-14}$ cm^3/erg are used for the resonant and non-resonant coupling, respectively. Gaussian pulses of 4.5 ps (laser) and 3 ps (Stokes) duration are assumed in accordance with our experimental conditions.

The situation for parallel polarization (case 1a of Fig. 1) is depicted in Fig. 2a. The resonant interaction via the isotropic part, a, of the scattering tensor dominates for $t_D > 0$, while the non-resonant part via χ_{NR} (broken curve) gives only a minor contribution to the total scattering signal $S^{coh}(t_D)$ (solid line). The signal curve decays slowly with a decay time $T_2/2$ representing the isotropic material excitation $|\langle Qs_1 \rangle|^2$. The effect of the orientational motion is insignificant because of the small anisotropy γ/a considered.

For crossed polarization (case 2a of Fig. 1) the signal transient is drasticly different. Here the resonant contribution to the scattering signal (dotted curve) originates from the small anisotropic part γ of the scattering tensor, which has only little effect on the total scattering signal $S^{coh}(t_D)$ (solid line) for small delay time. The non-resonant coupling via χ_{NR} dominates and generates a signal overshoot with rapid rise and decay around $t_D \simeq 0$. For larger values of t_D, the non-resonant part has disappeared and the signal curve decays with time constant $(2/T_2 + 2/\tau_R)^{-1}$; i.e. the anisotropic material excitation $|\langle Qs_2 \rangle|^2$ survives. A comparison of experimental data on the decay of $S_{\parallel}^{coh}$ and $S_{\perp}^{coh}$ for large t_D offers the possibility to determine the rotational time constant τ_R.

Experimental

Out theoretical results have been verified by an experimental investigation. The experimental system is schematically shown in Fig. 3. Single bandwidth-limited pulses are generated by a Nd:glass laser system, consisting of a mode-locked laser oscillator, pulse selector and amplifier stage and are subsequently

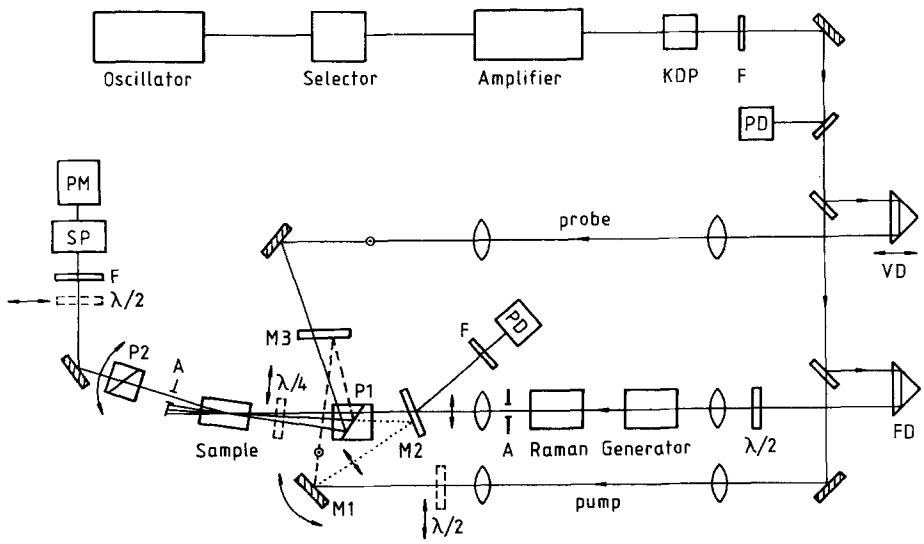

Fig. 3. Schematic of experimental set-up for coherent Raman probing with adjustable polarization conditions. Variable delay VD, fixed delay FD, photodetector PD, dielectric mirrors M1 to M3, polarizers P1 and P2, aperture A, filter F, spectrometer SP, photomultiplier PM

converted to the second harmonic by a KDP crystal. Passing a first beam splitter, 10% of the green laser pulse are removed to serve as a probing pulse with well-defined time delay. By the help of a second beam splitter, 50% of the remainder are directed into a Raman generator. Passing two liquid cells (length 5 cm) a Stokes shifted pulse builds up from quantum noise by high gain stimulated Raman scattering. CCl_4 and benzene are used to generate pulses of proper frequency position. The Stokes pulse and the rest of the green pulse are simultaneously directed into the sample cell (1–5 cm length). They serve for the excitation of the vibrational transition of interest by transient stimulated Raman scattering with small amplification factor and low scattering efficiency.

The coherent anti-Stokes scattering of the probe pulse is detected in a small solid angle of acceptance by a photomultiplier and a small grating spectrometer. Adjusting a well-defined off-axis geometry for the three input beams, k-matching of the probing process is achieved as calculated from available refractive index data. Crossed polarization planes are maintained in most of our experiments between the exciting Stokes and the probing pulse by the help of polarizer P1, while parallel (∥) or crossed (⊥) polarization can be adjusted for the input "laser" pulse with respect to the Stokes beam. This is achieved by two orientations of the mirror M_1 and two different dielectric mirrors M_2 and M_3, which alternatively direct the laser beam into the sample (Fig. 3). The polarization of the detected scattering signal is controlled by a second crossed polarizer P2 which is carefully rotated perpendicular with respect to the polarization plane of the green pump pulse in the different experiments. For part of our investigations more general polarization conditions are established by means of a $\lambda/4$ plate inserted in front of the sample cell. High quality components practically free of stress birefrigence are used achieving small transmission factors $\lesssim 10^{-5}$ through crossed polarizers.

Results and Discussion

The drastic change of the signal transients predicted for different polarizations has been observed experimentally. Figure 4 presents an example. The totally symmetric tetrahedron vibration ν_1 of neat CCl_4 at 459 cm^{-1} is investigated. The same substance is used in the Raman generator to produce a suitable Stokes shifted pump pulse. The data for parallel pump and probe polarization (∥, ∥) are depicted in Fig. 4a. The rapid increase and subsequent exponential decay of the scattering signal $S_{\parallel}(t_D)$ over nearly six orders of magnitude represent the time evolution of the isotropic material excitation. The vibrational dephasing time

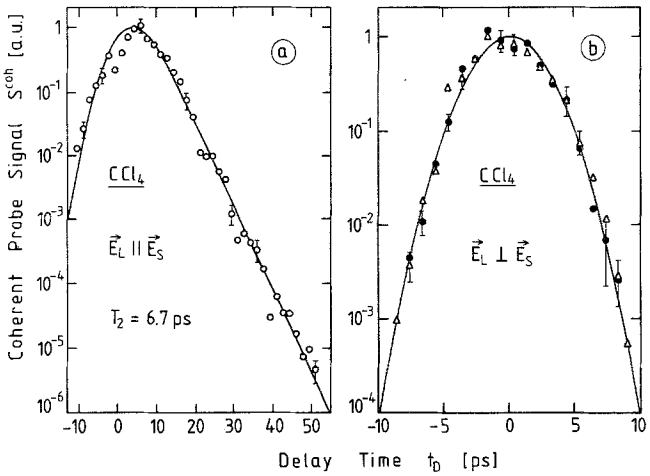

Fig. 4a and b. Coherent anti-Stokes scattering of CCl_4 vs. delay time: (a) parallel polarization (○); (b) crossed polarization (●); open triangles (△) refer to a C_6H_{12} sample with non-resonant excitation. Calculated curves assuming Gaussian pulses of 4.8 ps (laser) and 3.2 ps (Stokes) duration; $\chi_{NR}/\chi_{res}=0.016$ [15, 17]; $\gamma/a=0.19$ [14]

$T_2=6.7\pm0.6$ ps is directly obtained from the signal transient in good agreement with earlier results [2]. The solid line represents the calculated data obtained from the above theory. The isotopic multiplicity of the vibrational transition has been omitted in the computation for the sake of simplicity. Because of the small depolarization factor $\varrho_s\simeq0.0023$ [14] of the ν_1 mode corresponding to $\gamma^2/a^2\simeq0.035$ the effect of the orientational motion on the material excitation $\langle Qs_1\rangle$ via the correlation factor $\langle s_1 s_1\rangle$ is negligible, see (3, 4). Since the non-resonant contribution (parameter χ_{NR}) is also small [15], the resonant interaction via the isotropic part, a, of the Raman polarizability is dominant and the data of Fig. 4a represent purely vibrational dephasing, as noted previously [2].

Of particular interest are the data of Fig. 4b with rotated polarization plane of the green pump pulse and rotated polarizer P2 (crossed polarization). The observed coherent scattering $S_{\perp}^{coh}(t_D)$ is shown in the figure. We note a rapid increase and also decay of the scattering signal (full points). Because of the smallness of γ^2/a^2 and the short rotational time constant ($\tau_R=1.7$ ps [16]) the material excitations $\langle Qs_2\rangle$ and $\langle Qs_2\rangle_p$ are negligible and the contribution via the non-resonant part χ_{NRyzzy} dominates. For the Gaussian shape of our light pulses, the calculated signal transient (solid curve in Fig. 4b) is also Gaussian in good agreement with the experimental results (full points). Consistently we have measured the same time dependence replacing CCl_4 in the sample cell by C_6H_{12}, where the excitation process is far off resonance [6] (open triangles in Fig. 4b).

A comparison with the data of Fig. 4a gives information on the relative magnitude of the non-resonant

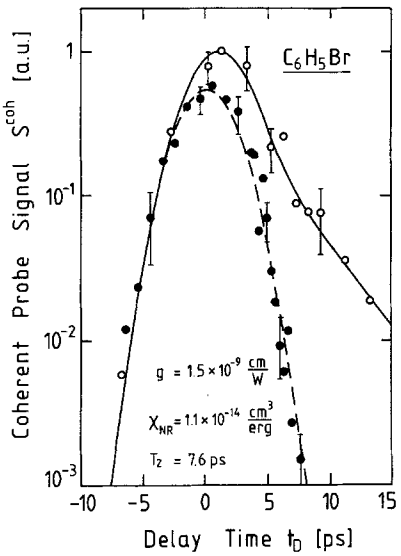

Fig. 5. Coherent anti-Stokes scattering of C_6H_5Br vs. delay time; full points (●): crossed polarization; open circles (○): more general polarization by $\lambda/4$-plate in front of the sample cell; theoretical curves calculated for the values of Fig. 2

and resonant contributions to the scattering process. For quantitative purposes we introduce the ratio χ_{NR}/χ_{res} where $\chi_{NR} = \chi_{NR\,yzzy}$ and [11]

$$\chi_{res} = \chi_{res\,yzyz} \simeq \tfrac{1}{2} N a \kappa_2 T_2 = c^2 \mu_L \mu_S g/(32\pi^2 \omega_S) \qquad (13)$$

(for $\gamma \lesssim a$; refractive indices $\mu_{L,S}$, steady-state gain factor g). From the measured ratio $S_\perp^{max}/S_\parallel^{max} \simeq 10^{-3}$ we estimate $\chi_{NR}/\chi_{res} \simeq 10^{-2}$ in satisfactory agreement with a value of 1.6×10^{-2}, which can be calculated from reported data for g [17] and χ_{NR} [15].

More accurate data on the ratio χ_{NR}/χ_{res} may be obtained when the two signal transients $S_\perp^{coh}(t_D)$ and $S_\parallel^{coh}(t_D)$ are measured with only minor changes of the experimental system. An example is shown in Fig. 5. The ring breathing mode of bromobenzene at 1000 cm^{-1} is investigated. As generator substance we use benzene (992 cm^{-1}). The observed scattering $S_\perp^{coh}(t_D)$ for crossed polarization is represented by the full points. We note a rapid rise and decay similar to Fig. 4b during the measured time interval of less than 8 ps in good agreement with the calculated curve. Also for the small depolarization factor $\varrho_s \simeq 0.04$ of the ring mode [18], the non-resonant contribution dominates. Now, a low-order $\lambda/4$ quartz plate (surface AR coated) is placed in front of the sample cell keeping the other experimental parameters constant. The specific plate [length: $3.25\,\lambda_L/(\mu_0 - \mu_e)$] generates circular polarization for the pump and probe fields E_L and E_p, while a well-defined elliptical polarization is produced for the input Stokes pulse. The adjusted experimental situation combines parallel and crossed polarization conditions discussed above (cases 1 and 2, Fig. 1). The measured scattering signal is indicated by the open circles in Fig. 5. We note a first rapid increase and decay of the signal curve, which receives large contributions from the non-resonant excitation: for larger values of t_D, the more slowly decaying resonant excitation $\langle Q s_1 \rangle$ survives which decreases according to the dephasing time T_2. The signal asymptote in Fig. 5 is consistent with the value of $T_2 = 7.4 \pm 0.5$ ps determined in an independent measurement with parallel polarization [19]. The solid line in Fig. 5 is calculated extending the theory discussed above to the more complex polarization conditions considered here; it represents a linear combination of $S_\perp^{coh}$ and $S_\parallel^{coh}$ and additional interference cross terms.

Comparison of the two signal curves of Fig. 5 allows to determine the non-resonant susceptibility. The ratio χ_{NR}/χ_{res} is the only fitting parameter for the computed signal transients in Fig. 5 which agree well with the experimental points. The result is $\chi_{NR}/\chi_{res} = 0.037 \pm 0.015$. Using the value for the steady-state gain factor $g = 1.5 \times 10^{-9}$ cm/W [20] for bromobenzene and (13) we arrive at $\chi_{NR} = (1.1 \pm 0.4) \times 10^{-14}$ cm^3/erg in satisfactory agreement with published data [13, 21, 15].

The theory discussed above predicts that a coherent scattering signal occurs either for parallel polarization ($\parallel, \parallel$) or for crossed polarization ($\perp, \perp$). For a mixed situation ($\parallel, \perp$ or $\perp, \parallel$) the scattering signal is expected to vanish. We have verified this result for the case $\perp, \parallel$ studying bromobenzene and also H_2O. No measurable scattering signal was detected; i.e., the signal level decreased by at least three orders of magnitude in comparison with crossed polarization ($\perp, \perp$).

In conclusion, we point out that we have investigated time-resolved coherent Raman scattering in liquids under generalized polarization conditions. Basic features of our theoretical treatment have been verified experimentally. The observed signal transients depend drastically on the chosen polarization geometry because of the varying role of different components of the involved material excitation.

References

1. See, for example, *Ultrafast Phenomena* IV, ed. by D. H. Auston, K. B. Eisenthal, Springer Ser. Chem. Phys. **38** (Springer, Berlin, Heidelberg 1984)
2. A. Laubereau, W. Kaiser: Rev. Mod. Phys. **50**, 3607 (1978)
3. D. von der Linde, A. Laubereau, W. Kaiser: Phys. Rev. Lett. **26**, 954 (1971)
4. R.R. Alfano, S.L. Shapiro: Phys. Rev. Lett. **26**, 1247 (1971) A. Laubereau, D. von der Linde, W. Kaiser: Phys. Rev. Lett. **27**, 802 (1971)
5. M.L. Geinaert, G.M. Gale, C. Flytzanis: Phys. Rev. Lett. **52**, 815 (1984)
6. W. Zinth, A. Laubereau, W. Kaiser: Opt. Commun. **26**, 457 (1978)

7. J. Kuhl, W.E. Bron: Solid State Commun. **49**, 935 (1984)
8. H. Graener, A. Laubereau, J.W. Nibler: Opt. Lett. **9**, 165 (1984)
9. For coherent Stokes scattering the situation is completely analogous
10. N. Kohles, A. Laubereau: To be published
11. A. Penzkofer, A. Laubereau, W. Kaiser: Prog. Quantum Electron. **6**, 55 (1979)
12. P.D. Maker, R.W. Terhune: Phys. Rev. **137**, A 801 (1965) see also M. Maier: Appl. Phys. **11**, 209 (1976)
13. M.D. Levenson, N. Bloembergen: Phys. Rev. B **10**, 4447 (1974)
14. W. Kiefer, J.A. Topp: Appl. Spectrosc. **28**, 26 (1974)
15. M.D. Levenson, N. Bloembergen: J. Chem. Phys. **60**, 1323 (1974)
16. F.J. Bartoli, T.A. Litovitz: J. Chem. Phys. **56**, 413 (1972)
17. H. Görner, M. Maier, W. Kaiser: J. Raman Spectr. **2**, 363 (1974)
18. J.G. Skinner, W.G. Nilsen: J. Opt. Soc. Am. **58**, 113 (1968)
19. K. Leupold: Diploma thesis, University of Bayreuth (1982)
20. W. Kaiser, M. Maier: In *Laser Handbook*, ed. by F. T. Arecchi, E. O. Schultz-Dubois (North-Holland, Amsterdam 1972)
21. S. Saikan, G. Marowsky: Opt. Commun. **26**, 466 (1978)